

THE STABILITY OF DILUTE PLASMAS WITH THERMAL AND COMPOSITION GRADIENTS. I. THE SLOW CONDUCTION LIMIT: OVERSTABLE GRAVITY MODES

MARTIN E. PESSAH AND SAGAR CHAKRABORTY

Niels Bohr International Academy, Niels Bohr Institute, Blegdamsvej 17, 2100 Copenhagen Ø, Denmark

Draft version November 16, 2011

ABSTRACT

We analyze the stability of a dilute plasma with thermal and composition gradients in the limit where conduction is slow compared to the dynamical timescale. We find necessary and sufficient conditions for stability when the background magnetic field is either parallel or perpendicular to the thermal and composition gradients that are parallel to the gravitational field. We provide approximate solutions for all the relevant modes involved, which are driven by gravity, conduction, and diffusion. We discuss the astrophysical implications of our findings for a representative galaxy cluster where helium has sedimented.

Subject headings: galaxies: clusters: intracluster medium — instabilities — magnetohydrodynamics

1. INTRODUCTION

Despite the fact that magnetic fields in galaxy clusters are too weak to be mechanically important, they can play a fundamental role in the dynamical stability of the dilute gas by channelling the transport of heat. The collision-less character of the hot intra-cluster medium (ICM), which is generically characterized by stable entropy gradients according to Schwarzschild's criterion (Piffaretti et al. 2005; Cavagnolo et al. 2009), enables the action of magnetic instabilities that are sensitive to temperature gradients (Balbus 2000, 2004). In particular, the magneto-thermal instability (MTI) operates when magnetic field lines are orthogonal to a temperature gradient parallel to the gravitational field (Balbus 2001), whereas the heat-flux-driven buoyancy instability (HBI) acts when magnetic field lines are parallel to a temperature gradient anti-parallel to the gravitational field (Quataert 2008). Numerical simulations suggest that the non-linear evolution of these instabilities leads to magnetic field configurations that tend to suppress the ability of the plasma to tap into the free energy supplied by the background temperature gradient (Parish et al. 2009; Bogdanović et al. 2009; Ruszkowski & Oh 2010). These magnetic field configurations can nevertheless support overstable gravity modes (Balbus & Reynolds 2010).

While the landscape of thermal instabilities that render homogeneous, dilute plasmas unstable has been well explored (Kunz 2011), and even extended to account for the effects of cosmic rays (Chandran & Dennis 2006), very little is known about the effects that composition gradients can have on the stability of the dilute ICM. If magnetic fields do not prevent the efficient diffusion of ions (Narayan & Medvedev 2001; Chuzhoy & Nusser 2003; Chuzhoy & Loeb 2004) then the gradients in mean molecular weight can be as important as the gradients in temperature (see Section 4 and Qin & Wu 2000; Peng & Nagai 2009; Shtykovskiy & Gilfanov 2010; Bulbul et al. 2011) and provide another source of free energy to feed instabilities. In order to obtain a more complete picture of the stability properties of the ICM, it is thus important to relax the assumption of a homogeneous plasma.

As a first step towards understanding the role of composition gradients in dilute plasmas, where magnetic fields play a key role by channelling the conduction of heat and the diffusion of ions, we investigate the stability of modes for which heat conduction is slow compared to the dynamical timescale involved. These modes contain, among others, the overstable g -modes studied by Balbus & Reynolds (2010).

2. MODEL FOR THE MULTICOMPONENT, DILUTE ATMOSPHERE

2.1. General Considerations for the Plasma Model

In order to highlight the physical phenomena that emerge when composition gradients are accounted for, we focus our attention on a dilute binary mixture (e.g., hydrogen and helium)¹ in a fixed gravitational field described by²

$$\frac{\partial \rho}{\partial t} + \nabla \cdot (\rho \mathbf{v}) = 0, \quad (1)$$

$$\frac{d\mathbf{v}}{dt} = -\frac{1}{\rho} \nabla \cdot \left(\mathbf{P} + \frac{\mathbf{B}^2}{8\pi} \mathbf{I} - \frac{B^2}{4\pi} \hat{\mathbf{b}}\hat{\mathbf{b}} \right) + \mathbf{g}, \quad (2)$$

$$\frac{\partial \mathbf{B}}{\partial t} = \nabla \times (\mathbf{v} \times \mathbf{B}), \quad (3)$$

$$\frac{P}{\gamma - 1} \frac{d}{dt} (\ln P \rho^{-\gamma}) = (p_{\perp} - p_{\parallel}) \frac{d}{dt} \ln \frac{B}{\rho^{\gamma-1}} - \nabla \cdot \mathbf{Q}_s, \quad (4)$$

$$\frac{dc}{dt} = -\nabla \cdot \mathbf{Q}_c. \quad (5)$$

Here ρ is the mass density, \mathbf{v} is the fluid velocity, \mathbf{B} is the magnetic field, \mathbf{g} is the gravitational acceleration, and γ is the adiabatic index. The Lagrangian and Eulerian derivatives are related via $d/dt \equiv \partial/\partial t + \mathbf{v} \cdot \nabla$.

Equations (1)–(5) describe the dynamics of a binary mixture in the low-collisionality regime and they differ from standard MHD in three important respects:

(i) The pressure tensor $\mathbf{P} \equiv p_{\perp} \mathbf{I} + (p_{\parallel} - p_{\perp}) \hat{\mathbf{b}}\hat{\mathbf{b}}$, is anisotropic; where the symbols \perp and \parallel refer to the directions perpendicular and parallel to the magnetic field, whose direction is given by the versor $\hat{\mathbf{b}} \equiv \mathbf{B}/B$.

(ii) Heat flows mainly along magnetic field lines, because the electron mean free path is large compared to its Larmor radius. This process is modeled by the second term on the right hand side of Equation (4) via $\mathbf{Q}_s \equiv -\chi \hat{\mathbf{b}}(\hat{\mathbf{b}} \cdot \nabla)T$, where T is the plasma temperature, assumed to be the same for ions and electrons, and $\chi \approx 6 \times 10^{-7} T^{5/2}$ ergs cm⁻¹ s⁻¹ K⁻¹ is the thermal conductivity (Spitzer 1962; Braginskii 1965).

¹ It is straightforward to generalize the present analysis to N species.

² For the sake of simplicity, we do not consider relatively weaker effects, such as thermo-diffusion, baro-diffusion, etc. (Landau & Lifshitz 1959).

(iii) The composition of fluid elements can change due to particle fluxes. Considering $\mathbf{Q}_c \equiv -D\hat{\mathbf{b}}(\hat{\mathbf{b}} \cdot \nabla)c$ on the right hand side of Equation (5) ensures that the diffusion of ions is mainly along magnetic field lines. This is a good approximation when the plasma is dilute enough for the ion mean free path to be large compared to the ion Larmor radius. Note that the concentration c is related to the mean molecular weight via $1/\mu \equiv (1-c)(1+Z_1)/\mu_1 + c(1+Z_2)/\mu_2$, where μ_i and Z_i , with $i = 1, 2$, are the molecular weights and the atomic numbers for the two ion species. The isotropic part of the pressure tensor is thus $P \equiv 2p_\perp/3 + p_\parallel/3 = \rho k_B T / \mu m_H$, where k_B is the Boltzmann constant and m_H is the atomic mass unit.

2.2. Background State and Equations for the Perturbations

We assume a plane-parallel atmosphere in a constant gravitational field $\mathbf{g} \equiv -g\hat{\mathbf{z}}$ which is stratified in both temperature and composition along the vertical direction. We consider a background magnetic field which is weak enough that the mechanical equilibrium of the atmosphere, with scaleheight H , is maintained via $dP/dz = -g\rho$. In general, the background heat and particle fluxes do not vanish, i.e., $\hat{\mathbf{b}} \cdot \nabla T \neq 0$ and $\hat{\mathbf{b}} \cdot \nabla c \neq 0$, unless the magnetic field and the background gradients are orthogonal. The existence of a well defined steady state, i.e., $\nabla \cdot \mathbf{Q}_s = \nabla \cdot \mathbf{Q}_c = 0$, demands that the background gradients should be linear functions of the distance along the direction of the magnetic field. However, even if this condition is not strictly satisfied, the dynamics of the modes that we consider is unlikely to be significantly affected if the local dynamical timescale is short compared to the timescale in which the entire system evolves (see also Quataert 2008).

The modes of interest have associated timescales that are long compared to the sound crossing time and it thus suffices to work in the Boussinesq approximation. In this limit, the equations for the linear perturbations $\delta \sim e^{\sigma t + i\mathbf{k} \cdot \mathbf{x}}$ become

$$\sigma \delta \mathbf{v} = -g \frac{\delta \rho}{\rho} \hat{\mathbf{z}} - i\mathbf{k} v_{\text{th}}^2 \left(\frac{\delta p_\perp}{P} + \frac{1}{\beta} \frac{\delta B_\parallel}{B} \right) + i k_\parallel v_A^2 \frac{\delta \mathbf{B}}{B} - \hat{\mathbf{b}} \frac{3k_\parallel^2 v_{\text{th}}^2}{2\nu} \delta v_\parallel, \quad (6)$$

$$\sigma \delta \mathbf{B} = i k_\parallel B \delta \mathbf{v}, \quad (7)$$

$$\sigma \frac{\delta \rho}{\rho} = \frac{N^2}{g} \delta v_z + \frac{\gamma - 1}{\gamma} \kappa k_\parallel^2 \frac{\delta T}{T} - i \frac{\gamma - 1}{\gamma} \kappa \mathbf{k} \cdot \left(\frac{d \ln T}{dz} \delta b_z \hat{\mathbf{b}} + b_z \frac{d \ln T}{dz} \frac{\delta \mathbf{B}_\perp}{B} \right), \quad (8)$$

$$\sigma \frac{\delta \mu}{\mu} = - \frac{d \ln \mu}{dz} \delta v_z - D k_\parallel^2 \frac{\delta \mu}{\mu} + i D \mathbf{k} \cdot \left(\frac{d \ln \mu}{dz} \delta b_z \hat{\mathbf{b}} + b_z \frac{d \ln \mu}{dz} \frac{\delta \mathbf{B}_\perp}{B} \right). \quad (9)$$

In agreement with the Boussinesq approximation, the velocity perturbations satisfy $\mathbf{k} \cdot \delta \mathbf{v} = 0$ and the fluctuations in density, temperature, and mean molecular weight are related via

$$\frac{\delta \rho}{\rho} + \frac{\delta T}{T} - \frac{\delta \mu}{\mu} = 0. \quad (10)$$

Here, we have introduced the Alfvén speed, $v_A \equiv B/\sqrt{4\pi\rho}$, the thermal speed, $v_{\text{th}} \equiv \sqrt{2P/\rho}$, the plasma $\beta \equiv v_{\text{th}}^2/v_A^2$, the viscosity ν of the binary mixture, the thermal diffusion

coefficient $\kappa \equiv \chi T/P$, and the Brunt–Väisälä frequency

$$N^2 \equiv \frac{g}{\gamma} \frac{d}{dz} \ln P \rho^{-\gamma} = g \frac{d}{dz} \ln \left(\frac{P^{\frac{1-\gamma}{\gamma}} T}{\mu} \right). \quad (11)$$

For completeness, we define here several quantities that play an important role in the stability analysis. We denote by $\omega_{\text{dyn}} \equiv (g/H)^{1/2}$ and $\omega_A \equiv \mathbf{k} \cdot \mathbf{v}_A$ the dynamical and Alfvén frequencies, respectively. The inverse time-scales $\tau_c^{-1} \equiv \kappa(\mathbf{k} \cdot \hat{\mathbf{b}})^2(\gamma - 1)/\gamma$, $\tau_d^{-1} \equiv D(\mathbf{k} \cdot \hat{\mathbf{b}})^2$, and $\tau_v^{-1} \equiv 3k_\parallel^2 v_{\text{th}}^2/2\nu$ characterize, respectively, the diffusion of heat, particles, and momentum along magnetic field lines. We also define two quantities which appear naturally when thermal and composition gradients are considered

$$N_{T\mu}^2 \equiv g \frac{d}{dz} \ln(T\mu), \quad N_{T/\mu}^2 \equiv g \frac{d}{dz} \ln \left(\frac{T}{\mu} \right). \quad (12)$$

3. LINEAR MODE ANALYSIS

We are concerned with modes for which heat conduction is slow compared to the dynamical timescale and thus $\omega_{\text{dyn}} \gg \tau_c^{-1}$. Because the timescales associated with viscous processes, which are comparable to those involved in diffusion, are longer than the conduction timescales by an order of magnitude (Kunz 2011), we also have $\tau_c^{-1} > \tau_v^{-1} \sim \tau_d^{-1}$. We further focus our attention on modes for which magnetic tension is unimportant, i.e., $k_\parallel H \ll \beta^{1/2}$, and thus the Alfvén frequency is small compared to other inverse timescales. Since the plasma β ranges from 10^2 from the centers of cool core clusters to 10^4 in the outskirts of the ICM (Carilli & Taylor 2002), there is a reasonable range of wavenumbers for which a local analysis is sensible. We can thus summarize the regime in which we are interested according to

$$\omega_{\text{dyn}} \gg \tau_c^{-1} > \tau_v^{-1} \sim \tau_d^{-1} \gg \omega_A. \quad (13)$$

For a homogeneous plasma, the modes satisfying these conditions encompass the overstable g -modes studied in Balbus & Reynolds (2010). The set of Equations (7)–(10) allows us to address the behavior of these, as well as other new modes, in the presence of a non-vanishing gradient in the mean molecular weight and account self-consistently for the diffusion of ions along magnetic field lines.

3.1. Heat Diffusion Along Vertical Magnetic Field Lines with No-Ion Diffusion

Let us first consider the case in which there is no ion diffusion. Setting $D = \nu = 0$ the dispersion relation corresponding to Equations (7) to (9) factorizes and possesses as non-trivial solutions two Alfvén waves, with $\sigma = \pm i\omega_A$, and the roots of the polynomial

$$\sigma^3 + a_1 \sigma^2 + a_2 \sigma + a_3 = 0, \quad (14)$$

with coefficients

$$a_1 = \tau_c^{-1}, \quad (15)$$

$$a_2 = \frac{k_\perp^2}{k^2} N^2 + \omega_A^2 \approx \frac{k_\perp^2}{k^2} N^2, \quad (16)$$

$$a_3 = -\tau_c^{-1} \left(\frac{k_\perp^2}{k^2} N_{T\mu}^2 - \omega_A^2 \right) \approx -\tau_c^{-1} \frac{k_\perp^2}{k^2} N_{T\mu}^2, \quad (17)$$

where the approximate expressions for the coefficients follow from the general considerations outlined above.

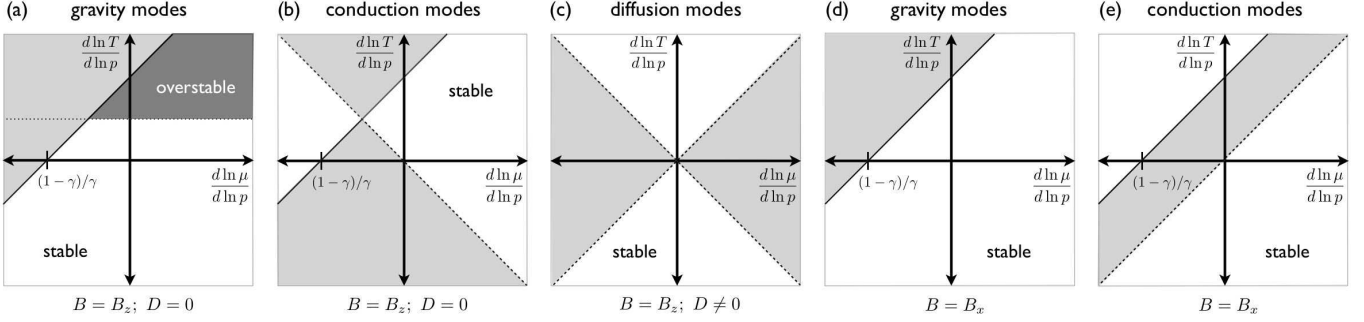


FIG. 1.— Graphic representation of the stability of modes for which conduction is slow compared to the dynamical timescale, i.e., $\omega_{\text{dyn}} \gg \tau_c^{-1}$. The various panels show the unstable regions (gray) for each of the modes that can be excited when the background magnetic field is parallel (a, b, and c) or perpendicular (d and e) to the background thermal and composition gradients. The solid line corresponds to $N^2 = 0$; the horizontal dotted line represents $d \ln T / d \ln P = (\gamma - 1) / 2\gamma$; and the dashed lines correspond to $d \ln T / d \ln P = \pm d \ln \mu / d \ln P$. For $B = B_z$, gravity modes (a) can become either stable or overstable, while modes driven by conduction can become unstable (b). If ions can diffuse efficiently along magnetic field lines, a new type of mode can become unstable (c). For $B = B_x$, both gravity modes (d) and conduction modes can become unstable (e); while ion diffusion only leads to decaying modes.

The Routh–Hurwitz stability criteria that predict exclusively negative real parts for the roots of the cubic Equation (14) are: $a_1 > 0$, $a_3 > 0$, and $a_1 a_2 - a_3 > 0$. The first condition is trivially satisfied while the other two imply

$$N_{T\mu}^2 < 0, \quad (18)$$

$$N^2 + N_{T\mu}^2 > 0, \quad (19)$$

respectively. To leading order, two of the solutions of Equation (14) are given by $\sigma \approx \pm i a_2^{1/2} + (a_3 - a_1 a_2) / 2 a_2$, i.e.,

$$\sigma \approx \pm i \frac{k_{\perp}}{k} \sqrt{N^2} - \frac{1}{2\tau_c} \left(1 + \frac{N_{T\mu}^2}{N^2} \right), \quad (20)$$

which correspond to gravity modes. In the absence of a gradient in the mean molecular weight, these reduce to the g -modes discussed in Balbus & Reynolds (2010). The third root is given by $\sigma \approx -a_3 / a_2$, i.e.,

$$\sigma \approx \tau_c^{-1} \frac{N_{T\mu}^2}{N^2}, \quad (21)$$

and corresponds to a mode driven by conduction. Assuming that $N^2 > 0$, g -modes are overstable if the condition (19) is not satisfied, while conduction modes are unstable if (18) is not fulfilled.

In order to understand how these modes behave in the parameter space spanned by temperature and composition gradients, it is convenient to use that $d \ln P / dz = -1/H$ and work with the dimensionless variables $d \ln T / d \ln P$ and $d \ln \mu / d \ln P$. The classical requirement for stability against buoyancy, i.e., $N^2 > 0$ becomes

$$\frac{d \ln T}{d \ln P} < \frac{d \ln \mu}{d \ln P} + \frac{\gamma - 1}{\gamma}, \quad (22)$$

while the conditions (18) and (19) become, respectively,

$$\frac{d \ln T}{d \ln P} > -\frac{d \ln \mu}{d \ln P}, \quad (23)$$

$$\frac{d \ln T}{d \ln P} < \frac{\gamma - 1}{2\gamma}. \quad (24)$$

The first panel (a) in Figure 1 shows the regions of parameter space where g -modes in Equation (20) are stable, overstable, or unstable (gray area). The second panel (b) shows that the modes in Equation (21), which are driven by conduction, can

be either stable or unstable. Note that in the region of parameter space where both gravity and conduction modes are overstable/unstable they both grow with comparable rates. Panel (a) in Figure 2 shows the stable region (white) of parameter space satisfying the conditions (23) and (24) simultaneously.

3.2. Heat and Ion Diffusion Along Vertical Magnetic Field Lines

Let us now consider the situation in which ions diffuse mainly along magnetic field lines. If $D \neq 0$, the dispersion relation corresponding to Equations (7) to (9) yields as non-trivial roots $\sigma = \pm i \omega_A$ and the solutions to

$$\sigma^4 + b_1 \sigma^3 + b_2 \sigma^2 + b_3 \sigma + b_4 = 0, \quad (25)$$

with coefficients

$$b_1 = \tau_c^{-1} + \tau_d^{-1} + \frac{k_{\perp}^2}{k^2} \tau_v^{-1} \approx \tau_c^{-1},$$

$$b_2 = \frac{k_{\perp}^2}{k^2} N^2 + \omega_A^2 + \tau_c^{-1} \left(\tau_d^{-1} + \frac{k_{\perp}^2}{k^2} \tau_v^{-1} \right) \approx \frac{k_{\perp}^2}{k^2} N^2, \quad (26)$$

$$b_3 = -\tau_c^{-1} \left[\frac{k_{\perp}^2}{k^2} N_{T\mu}^2 - \omega_A^2 \right] + \tau_d^{-1} \left[\frac{k_{\perp}^2}{k^2} (N^2 + \tau_c^{-1} \tau_v^{-1}) + \omega_A^2 \right]$$

$$\approx -\tau_c^{-1} \frac{k_{\perp}^2}{k^2} N_{T\mu}^2, \quad (27)$$

$$b_4 = -\tau_d^{-1} \tau_c^{-1} \left[\frac{k_{\perp}^2}{k^2} N_{T/\mu}^2 - \omega_A^2 \right] \approx -\tau_d^{-1} \tau_c^{-1} \frac{k_{\perp}^2}{k^2} N_{T/\mu}^2. \quad (28)$$

The approximations on each of the last terms on the right hand side hold under the same considerations that lead to the simplified coefficients a_i in Section 3.1. The approximate expressions for the coefficients b_i and a_i are identical for $i = 1, 2, 3$.

The Routh–Hurwitz stability criteria for a quartic polynomial with real coefficients requires: $b_1 > 0$, $b_4 > 0$, $b_1 b_2 - b_3 > 0$, and $b_1 b_2 b_3 - b_1^2 b_4 - b_3^2 > 0$. While $b_1 > 0$ is trivially satisfied, $b_4 > 0$ implies:

$$N_{T/\mu}^2 < 0. \quad (29)$$

The other two conditions lead again to inequalities (18) and (19). Therefore, the effects of diffusion require that only the additional condition (29) be met for the system to be stable.

To leading order, three of the roots of the dispersion relation (25) are given by Equations (20) and (21). The fourth solution

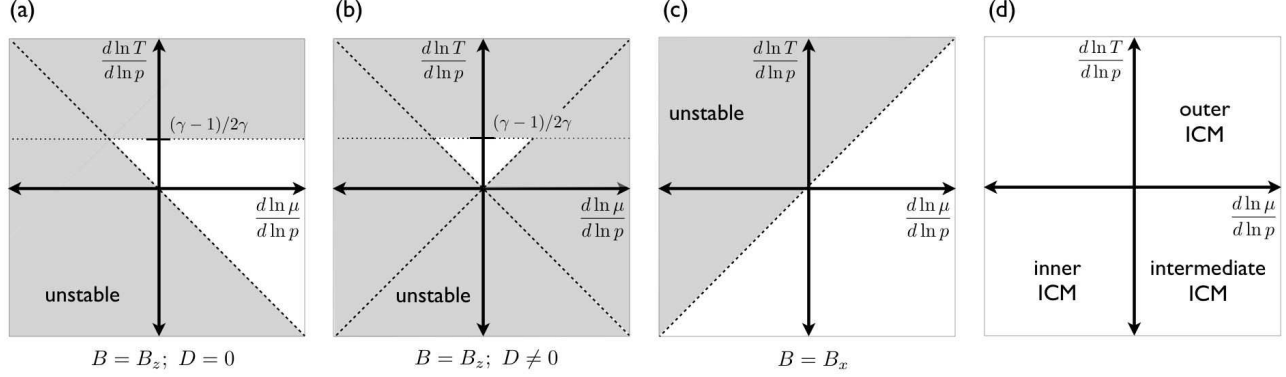


FIG. 2.— Panels (a), (b), and (c) show a graphic representation of the stable regions (white) satisfying all the Routh–Hurwitz stability criteria discussed in Section 3. Panel (d) is a schematic representation of the correspondence between the regions of a representative galaxy cluster with radial temperature and mean molecular weight profiles as shown in Figure 3 and the plane spanned by $(d \ln T / d \ln P, d \ln \mu / d \ln P)$.

consists of a mode driven by ion diffusion

$$\sigma \approx -\tau_d^{-1} \frac{N_{T/\mu}^2}{N_{T\mu}^2}. \quad (30)$$

This is an unstable mode if either of the criteria (18) or (29) is unfulfilled.

Thus, if ions can diffuse along magnetic field lines, in addition to requiring that the gradients in temperature, pressure, and mean molecular weight satisfy the inequalities (23) and (24), we must have

$$\frac{d \ln T}{d \ln P} > \frac{d \ln \mu}{d \ln P}. \quad (31)$$

The third panel (c) in Figure 1 shows that the modes in Equation (30), which are driven by diffusion, can be either stable or unstable (gray). Their growth rates are estimated to be an order of magnitude smaller than either g -modes or conduction modes. The importance of these diffusion modes resides in that they can become unstable in regions of parameter space which are stable against g -modes and conduction modes. Panel (b) in Figure 2 shows the stable region (white) of parameter space satisfying all the conditions (23), (24), and (31) simultaneously.

3.3. Heat and Ion Diffusion Along Horizontal Magnetic Field Lines

If the background magnetic field is perpendicular to the thermal and composition gradients, the dispersion relation that governs the stability of the atmosphere is ³

$$\sigma^5 + c_1 \sigma^4 + c_2 \sigma^3 + c_3 \sigma^2 + c_4 \sigma + c_5 = 0, \quad (32)$$

where the coefficients

$$c_1 \approx \tau_c^{-1} + \tau_v^{-1} \frac{k_\perp^2}{k^2}, \quad (33)$$

$$c_2 \approx N^2 \frac{k_x^2 + k_y^2}{k^2} + \tau_c^{-1} \tau_v^{-1} \frac{k_\perp^2}{k^2}, \quad (34)$$

$$c_3 \approx \tau_c^{-1} N_{T/\mu}^2 \frac{k_x^2 + k_y^2}{k^2} + \tau_v^{-1} N^2 \frac{k_y^2}{k^2}, \quad (35)$$

$$c_4 \approx \tau_c^{-1} \tau_v^{-1} N_{T/\mu}^2 \frac{k_y^2}{k^2}, \quad (36)$$

³ In the absence of diffusion, the only result that is modified in this section is that the root $\sigma = -\tau_d^{-1}$ for $D \neq 0$ becomes $\sigma = 0$ for $D = 0$.

$$c_5 \approx \omega_A^2 \tau_c^{-1} N_{T/\mu}^2 \frac{k_x^2 + k_y^2}{k^2}, \quad (37)$$

are subject to the same considerations employed in deriving the approximate expressions for the coefficients a_i and b_i .

The Routh–Hurwitz stability criteria for a fifth degree polynomial requires $c_1 > 0$, $c_1 c_2 - c_3 > 0$, $c_1 c_2 c_3 - c_1^2 c_4 - c_3^2 + c_1 c_5 > 0$, $c_4(c_1 c_2 c_3 - c_1^2 c_4 - c_3^2) > c_5(c_1 c_2^2 - 2c_1 c_4 - c_2 c_3 + c_5)$, and $c_5 > 0$. In the limit under consideration, i.e., $\omega_{\text{dyn}} \gg \tau_c^{-1} > \tau_v^{-1}$, these inequalities become, respectively,

$$\tau_c^{-1} > 0, \quad (38)$$

$$N^2 - N_{T/\mu}^2 > 0, \quad (39)$$

$$N_{T/\mu}^2 (N^2 - N_{T/\mu}^2) > 0, \quad (40)$$

$$(N_{T/\mu}^2)^2 (N^2 - N_{T/\mu}^2) > 0, \quad (41)$$

$$N_{T/\mu}^2 > 0. \quad (42)$$

The first of these conditions is trivially satisfied. This is also the case for inequality (39), since it can be written as $[(\gamma - 1)/\gamma][dP/dz]^2/P\rho > 0$. Therefore, the only independent condition required for stability is $N_{T/\mu}^2 > 0$.

Two of the approximate solutions to the dispersion relation (32) are given by $\sigma \approx \pm i c_2^{1/2} + (c_3 - c_1 c_2)/2c_2$, i.e.,

$$\sigma \approx \pm i \frac{\sqrt{k_x^2 + k_y^2}}{k} \sqrt{N^2} - \frac{1}{2\tau_c} \left(1 - \frac{N_{T/\mu}^2}{N^2} \right), \quad (43)$$

which correspond to stable gravity modes. The other two solutions correspond to a conduction and a viscous (decaying) mode, which are, respectively

$$\sigma \approx -\tau_c^{-1} \frac{N_{T/\mu}^2}{N^2}, \quad \sigma \approx -\tau_v^{-1} \frac{k_y^2}{k_x^2 + k_y^2}. \quad (44)$$

We conclude that when the magnetic field is perpendicular to the temperature and composition gradients, the stability of g -modes requires only that $N^2 > 0$, whereas the stability of conduction modes requires also

$$\frac{d \ln T}{d \ln P} < \frac{d \ln \mu}{d \ln P}. \quad (45)$$

The fourth panel (d) in Figure 1 shows the regions of parameter space where g -modes in Equation (43) are stable or

unstable (gray). The fifth panel (e) shows that the modes in Equation (44), which are driven by conduction, can be either stable or unstable. These regions are significantly different from the corresponding regions in panel (b), for which the direction of the background magnetic field is parallel to the direction of the temperature and composition gradients. Note that, unlike the case where $B = B_z$, g -modes and conduction modes cannot be simultaneously unstable when $B = B_x$. Panel (c) in Figure 2 shows the stable region (white) of parameter space satisfying the condition (45).

4. ASTROPHYSICAL IMPLICATIONS

We have provided a detailed description of the various instabilities that can be present in the parameter space spanned by $(d \ln T / d \ln P, d \ln \mu / d \ln P)$ without imposing restrictions on the relative signs of the gradients involved. We can now frame our results, summarized in Figure 2, in the context provided by observations and theoretical models addressing the temperature and composition structure of galaxy clusters. Figure 3 shows a schematic representation of the temperature and mean molecular weight profiles of a representative galaxy cluster. The temperature profile sketched there resembles the results obtained by observations (Vikhlinin et al. 2006), whereas the mean molecular weight profile is akin to helium sedimentation models (Bulbul et al. 2011). If the peak in the temperature takes place at a larger radius than the peak in the mean molecular weight, then there are three distinct regions defined by the signs of the temperature and composition gradients. These regions correspond to different quadrants in the $(d \ln T / d \ln P, d \ln \mu / d \ln P)$ plane as shown in panel (d) in Figure 2.

The joint analysis of Figures 1 and 2 allows us to understand the implications that mean molecular weight gradients can have for the various regions of a representative galaxy cluster as depicted in Figure 3. If the magnetic field in the inner ICM is perpendicular to the background temperature gradient $dT/dz > 0$, as suggested by the end states of initial configurations with $B = B_z$ that are HBI-unstable but evolve to $B \approx B_x$, then this region is stable if $d\mu/dz = 0$ (although there could be overstable g -modes driven by radiative cooling Balbus & Reynolds 2010). However, if $d\mu/dz > 0$ this region is unstable to conduction modes. If the magnetic field in the outer ICM is parallel to the temperature gradient $dT/dz < 0$, as suggested by the end states of initial configurations with $B = B_x$ that are MTI-unstable but evolve to $B \approx B_z$, then this region is overstable to g -modes and unstable to conduction modes even if $d\mu/dz = 0$. A negative gradient in the

mean molecular weight is unable to stabilize these modes and it can further drive unstable diffusion modes. Therefore, even if the outer/inner ICM is stable to both the MTI and the HBI, it could be rendered unstable to modes driven by either gravity, conduction, or diffusion. Unless the magnetic field is orthogonal to the background gradients, the region that we have denoted as intermediate is likely to be unstable to conduction and diffusion modes, but not to gravity modes. These g -modes, however, could be relevant if the temperature profile peaks at a smaller radius than the mean molecular weight profile.

We will address the limit in which conduction is fast compared to the dynamical timescale in a forthcoming paper. This limit contains the generalization of the instabilities that become the MTI and the HBI in the limit of a homogeneous plasma.

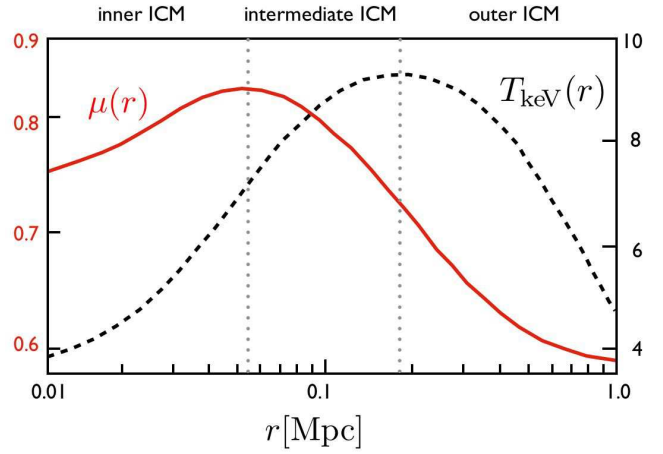


FIG. 3.— Schematic representation of the mean molecular weight (red solid line) and temperature (black dashed line) profiles of a representative galaxy cluster as suggested by observations (Vikhlinin et al. 2006) and theoretical models (Bulbul et al. 2011). The regions denoted by “inner”, “intermediate”, and “outer” ICM (delimited by dotted gray lines) correspond to three different quarters in the $(d \ln T / d \ln P, d \ln \mu / d \ln P)$ plane (Fig. 2.). The mean molecular weight for a homogeneous cluster with primordial abundance is $\mu \approx 0.59$.

We thank Matthew Kunz, Aldo Serenelli, and Shantanu Mukherjee for useful discussions. MEP is grateful to the Knud Højgaard Foundation for its generous support. SC acknowledges support from the Danish Research Council through FNU Grant No. 505100-50 - 30,168.

REFERENCES

- Balbus, S. A. 2000, *ApJ*, 534, 420
—, 2001, *ApJ*, 562, 909
—, 2004, *ApJ*, 616, 857
Balbus, S. A., & Reynolds, C. S. 2010, *ApJ*, 720, L97
Bogdanović, T., Reynolds, C. S., Balbus, S. A., & Parrish, I. J. 2009, *ApJ*, 704, 211
Braginskii, S. I. 1965, *Reviews of Plasma Physics*, 1, 205
Bulbul, G. E., Hasler, N., Bonamente, M., Joy, M., Marrone, D., Miller, A., & Mroczkowski, T. 2011, *A&A*, 533, A6
Carilli, C. L., & Taylor, G. B. 2002, *ARA&A*, 40, 319
Cavagnolo, K. W., Donahue, M., Voit, G. M., & Sun, M. 2009, *ApJS*, 182, 12
Chandran, B. D., & Dennis, T. J. 2006, *ApJ*, 642, 140
Chuzhoy, L., & Loeb, A. 2004, *MNRAS*, 349, L13
Chuzhoy, L., & Nusser, A. 2003, *MNRAS*, 342, L5
Kunz, M. W. 2011, *MNRAS*, 417, 602
Landau, L. D., & Lifshitz, E. M. 1959, *Fluid mechanics*, ed. Landau, L. D. & Lifshitz, E. M.
Narayan, R., & Medvedev, M. V. 2001, *ApJ*, 562, L129
Parrish, I. J., Quataert, E., & Sharma, P. 2009, *ApJ*, 703, 96
Peng, F., & Nagai, D. 2009, *ApJ*, 693, 839
Piffaretti, R., Jetzer, P., Kaastra, J. S., & Tamura, T. 2005, *A&A*, 433, 101
Qin, B., & Wu, X.-P. 2000, *ApJ*, 529, L1
Quataert, E. 2008, *ApJ*, 673, 758
Ruszkowski, M., & Oh, S. P. 2010, *ApJ*, 713, 1332
Shtykovskiy, P., & Gilfanov, M. 2010, *MNRAS*, 401, 1360
Spitzer, L. 1962, *Physics of Fully Ionized Gases*, ed. Spitzer, L.
Vikhlinin, A., Kravtsov, A., Forman, W., Jones, C., Markevitch, M., Murray, S. S., & Van Speybroeck, L. 2006, *ApJ*, 640, 691